J. Water Environ. Nanotechnol., 7(4): 407-427 Autumn 2022

ORIGINAL RESEARCH PAPER

Scrutinizing The Applications Of Mangrove Actinomycetes Mediated Biosynthesized Copper Nanoparticles

Ravindra Ashok Sharma[1*], Prajakta Kashinath Jagtap[2]

[1] Department of Microbiology, Ramchand Kimatram Talreja College, Ulhasnagar- 421003, Maharashtra, India
[2] Department of Basic and Applied Science, National Institute of Food Technology Entrepreneurship and Management, Sonipat-131028, Haryana, India

Received: 2022-08-08 Accepted: 2022-09-03 Published: 2022-10-01

ABSTRACT

Recently, there has been an increase in research interest in metal nanoparticles and their synthesis because of their various applications in different industrial areas. The current study deals with the Actinomycetes-mediated synthesis of copper nanoparticles (CuNPs) isolated from mangrove soil and to further access its application in different fields. Eight different soil samples were collected from three different mangrove sites located in Mumbai. A total of 15 different Actinomycetes isolates were obtained from soil samples and studied in the present investigation and were screened for metal tolerance. It was found that out of 15 isolates, only 3 were able to tolerate the highest metal salt concentration i.e. 10^{-1}M. The synthesized CuNPs were further investigated with various characterizations such as UV-Vis spectroscopy, FTIR, and XRD. The identification of isolate GRC1 was done as per Bergey's Manual of Systematic Bacteriology Volume 5 for preliminary identification of Actinomycetes and was identified as *Streptomyces* sp. This isolate was further characterized by Vitek MS and it was identified as *Streptomyces verticillus.* The inhibition zone by biosynthesized CuNPs was significantly greater when compared with standard antibiotics and CuSO4. The calculated degradation efficiency after 5hrs of incubation was 59.67% and 96.26% for Red M8B and Reactive green, respectively. Prevention of biofilm formation by CuNPs was confirmed by microscopic technique and significant inhibition of biofilm was observed. Thus, the mangrove Actinomycetes mediated bio-fabrication of CuNPs should gain much attention because of their unique properties like antimicrobial, anticancer, catalytic activity, wound healing, and antifouling.

Keywords: *Copper Nanoparticles, Actinomycetes, Mangroves, Biosynthesis, Antimicrobial, Dye Degradation, Antifouling*

How to cite this article
Ashok Sharma R., Kashinath Jagtap P. Scrutinizing The Applications Of Mangrove Actinomycetes Mediated Biosynthesized Copper Nanoparticles. J. Water Environ. Nanotechnol., 2022; 7(4): 407-427.
DOI: 10.22090/jwent.2022.04.007

INTRODUCTION

Nanomaterials prepared from earth-abundant and inexpensive metals have attracted considerable attention because of their potential as viable alternatives to the rare and expensive noble metal catalysts used in many conventional commercial chemical processes [1]. These metal NPs often exhibit activity different from that of the corresponding bulk materials because of their different sizes and shapes, which give rise to distinctive quantum properties. Since copper resembles the properties of gold and silver according to the periodic table, it can be used as an alternative cheap nanoparticle to the expensive gold and silver nanoparticles [2,3]. Copper has several distinct properties in synthesizing as it can easily be oxidized at room temperature. Also copper is a more promising material due to its abundance in nature and low cost. In comparison,

* Corresponding Author Email: *ravindrasharma2198@gmail.com*

with noble metals such as Silver, Platinum, and Gold, Copper is a cheap material however it is also accountable for oxidation generally in nanoscale dimensions. Copper nanoparticles have various properties like catalytic, anti-microbial, antifungal, and anti-cancerous.

However, the main concern is the synthesis methods, which result in stable nanoparticles. Green synthesis has been an extremely focused area in the field of nanotechnology and has been employed for enzymatic and non-enzymatic production of copper nanoparticles. In the past, scientist and researchers tried their best to discover new methods for the synthesis of metal nanoparticles. One of the breakthroughs was the discovery of the "Biosynthesis" approach. The biosynthesis of copper nanoparticles using plant extracts and microbial agents such as bacteria, fungi, etc. has received tremendous attention in the area of nanotechnology for the past few years [4].

The biosynthesis of nanoparticles has been reported by using unicellular and multicellular organisms like *Actinomycetes*, bacteria, fungi, marine algae, plants, viruses, and yeasts exist as successful candidates. *Actinomycetes* are an efficient candidate for the synthesis of metal nanoparticles as they exhibit good stability and polydispersity [5]. The studies on the biosynthesis of nanoparticles from *Actinomycetes* are limited and should be scrutinized more. The mangrove ecosystem comprises different kinds of extreme environmental conditions and can be explored for the discovery of new bioactive metabolites [6]. Thus, the aim of the current study deals with the synthesis of copper nanoparticles from *Actinomycetes* isolated from mangrove soil and to further access its application in different fields.

MATERIALS AND METHODS

Collection of soil sample

Eight different soil samples were collected from three different mangrove sites located in Mumbai. The soil samples were collected from the following sites a) Gorai beach located in Borivali (19.250057°N, 72.782021°E), b) Godrej Mangroves located in Vikhroli (19.324282˚N, 72.5775348˚E), c) Diva Mangroves located in Diva (19°8'47"N 72°59'30"E). Soil samples were collected from a depth of 10 - 15 cm aseptically, labeled, and brought to the laboratory in sterile plastic containers. The soil samples were then air-dried for a week and kept at 45˚C for 1hr to minimize the bacterial contaminants [7].

Isolation of Actinomycetes

After drying soil samples for a week it was passed through a 2mm sieve and then 1g of the soil sample was taken and transferred to a 150mL Erlenmeyer's flask containing 99mL sterile saline. The sample suspension was serially diluted up to 10^{-5} dilution and about 0.1mL was then spread onto AIA (Actinomycetes Isolation Agar) (Sodium caseinate - 2.0g/L, L- Asparagine - 0.1g/L, Sodium propionate - 4.0g/L, Dipotassium phosphate- 0.5g/L, Magnesium sulfate - 0.1g/L, Ferrous sulfate - 0.001g/L, Agar - 15g/ L adjusted to a final pH of 8.1 ± 0.2), SCA (Starch Casein Agar) (Starch – 10g/L, Casein powder 1g/L, Seawater 37g/L, Agar – 15g/L adjusted to a final pH of 7.2 ± 0.2), and SNA (Starch Nitrate Agar) (Starch – 20g/L, KNO_3 – 2g/L, K_2HPO_4 – 1g/L, $MgSO_4.7H_2O$ - 0.5g/L, and Agar – 20g/L adjusted to a final pH of 7.0 ± 0.2) plates [8].

The AIA and SCA plates were then incubated at 27° C for 7 – 14 days. At the end of the incubation, plates were observed for *Actinomycetes* growth and the strains of *Actinomycetes* were picked out and purified by repeated streaking on AIA and SCA. The isolated colonies were further sub-cultured and pure colonies were transferred on Glycerol asparagine agar it was labeled and incubated at room temperature for 7-14 days. After incubation, the slants were maintained at 4° C until further use [9].

Maintenance of cultures

Stock cultures were maintained by periodic transfer on Glycerol asparagine agar (GAA) medium supplemented with antifungal griseofulvin (50µg/mL), at 2-week intervals [10].

Screening of Actinomycetes for metal tolerance

The heavy metal tolerance limit of all isolated *Actinomycetes* was tested in a minimal medium with various concentrations of metal viz. 10^{-9} M, 10^{-7} M, 10^{-5} M, 10^{-3} M, and 10^{-1} M. $AgNO_3$, $MnSO_4$, $CuSO_4$, and $ZnSO_4$, metal salts were used for testing the tolerance of isolated *Actinomycetes* [11]. 0.5ml of inoculum was inoculated in 10 mL sterilized Glycerol asparagine broth (GAB) containing metal salts at various concentrations taken in a tube and incubated at 35 □ for 5 days. The growth in the tube was considered as a tolerance to the specific metal [12]. It was compared with positive and negative control. Positive control was prepared by inoculating Actinomycetal inoculum in Glycerol

asparagine broth and negative control was Glycerol asparagine broth without inoculation. The metal tolerance was noted as follows by observing growth in the tube.

-No growth (sensitive), + Growth (resistant). Metal-resistant *Actinomycetes* were selected for further studies.

Bio-fabrication of copper nanoparticles

Actinomycete isolates exhibiting metal resistance were used for biosynthesis of copper nanoparticles as follows: *Actinomycetes* strains were inoculated in a 250 mL flask containing Tryptone Yeast Extract Broth (Casein hydrolysate – 5g/L, Yeast extract – 3g/L with a final pH of 7.2 ± 0.2) (ISP Medium No. 1). The flasks was kept in the rotary shaker and incubated at 28° C for 7 days [13]. After the incubation period, the cell-free supernatant (CFS) was collected by centrifugation at 10,000 rpm and the supernatant obtained was then used for the synthesis of copper. About 25 mL of the cell-free supernatant was mixed with an aqueous solution of 10 mM copper sulfate [$CuSO_4$. $5H_2O$] and then heated at 100° C for 15 min, resulting in the color change from blue to reddish-brown.

After the color change was observed the suspension was subjected to centrifugation at 10,000 rpm for 15 min, and the copper nanoparticles (CuNPs) were then obtained. The pellet was washed repeatedly with distilled water and centrifuged again for 10 min, then followed by ethanol wash to remove the water-soluble molecules from the CuNPs suspension. The copper oxide nanoparticles were then dried at 100° C and stored in an airtight container until further analysis of nanoparticles [14].

Identification of Actinomycetes

The following factors were considered for the identification of Actinomycetal isolates:

Colony characteristics

To study colonial characteristics, the isolates were inoculated on Bennet's agar and the plates will then be incubated for five days at ambient temperature. The colony characters of well-isolated colonies were studied.

Pigmentation

The pigmentation character of isolates was studied on glycerol asparagine agar [15] in terms of

a. Shade: Colony pigmentation was observed for various shades such as blue, violet, red, rose yellow, green-brown, and black.

b. Diffusible and Non-diffusible pigments.

c. Colony reverses: Yellow, brown (no distinctive pigment), blue, green, red, orange, or violet color.

Microscopic characteristics

The samples were prepared by the method given by Li *et al*., [16]. The coverslip culture of *Actinomycete* isolates was prepared for morphological characteristics such as aerial mycelium, substrate mycelium, and sporulation.

A sterilized coverslip was carefully inserted at an angle of 45° into a solidified medium in a Petri dish so that half of the coverslip is in the medium. An inoculum from a slope culture was then spread along the line, where the upper surface of the coverslip meets the agar with the nichrome wire loop. Plates were then incubated at room temperature for 5 days. Then coverslip was carefully withdrawn from the medium and placed in an upward position on a slide and observed under a high-power microscope. The microscopic observations like the presence and absence of aerial mycelium, substrate mycelium, sclerotia or sporangia, fragmentation of the substrate mycelium, and sporulation of substrate mycelium and spore chain morphology were studied using the coverslip culture technique.

Biochemical characteristics

Biochemical studies were carried out for the identification of *Actinomycetes* isolates as follows-

Utilization of carbon sugar

The inoculum was spot inoculated on the carbon utilization medium with 1% (w/v) of a specific carbon source [17]. The presence of growth on the medium after incubation at 35 °C for 5 days indicates a positive test.

H_2S production test

The ability of the isolates to produce hydrogen sulfide was tested by inoculating isolates into peptone nitrate broth. The lead acetate strips were inserted into the necks of culture tubes [18]. The tubes were then incubated at 35°C for 7 days; the blackish color of lead acetate paper is to be recorded as a positive test.

Catalase test

A clean glass slide was taken and a drop of

culture suspension was placed on it. A few drops of hydrogen peroxide were then added to the culture. The evolution of air bubbles from the suspension indicated a positive reaction [19].

Study of enzyme activity

The isolates were inoculated on the suitable nutrient medium by spot inoculation method in order to check different enzymatic degradation activities. The plates or tubes were incubated at 35° C for 7 days. The details are given in the table below

The potent isolates were further characterized by using VITEK MS System. Characterization was performed according to the manufacturer's instructions (VITEK MS System, Biomerieux Inc.). An unknown bio pattern was compared to the database of reactions for each taxon, and a numerical probability calculation was performed. Various qualitative levels of identification were assigned based on the numerical probability calculation [20].

Test data from an unknown organism were compared to the respective database to determine a quantitative value for proximity to each of the database taxa. Each of the composite values was compared to the others to determine if the data are sufficiently unique or close to one or more of the other database taxa. If a unique identification pattern is not recognized, a list of possible organisms is given, or the strain is determined to be outside the scope of the database [21].

Characterization of metal nanoparticles

The UV-Visible absorption spectra were recorded in the wavelength range of 400 nm – 750nm employing UV-2400 series UV-Visible spectroscopy in diffuse reflectance mode using distilled water as a reference. Spectra were recorded at room temperature [22].To identify the possible functional groups involved in the synthesis of nanoparticles FTIR analysis (Agilent Cary 630 FTIR Spectrometer) was performed the infrared spectra were measured in the wavelength range of 4000 – 600 cm^{-1}.

Applications of copper nanoparticles

Antimicrobial activity

Bacterial sensitivity to antibiotics is commonly tested using a disk diffusion test, employing antibiotic-impregnated disks. A similar test with nanoparticle-laden disks was used in this study [23]. Antagonistic activity of biosynthesized CuNPs was assessed against prokaryotic and eukaryotic test organisms represented by Gram-positive bacteria (*Staphylococcus aureus* ATCC.25923, *Enterococcus faecalis* ATCC.29212), Gram-negative bacteria (*Salmonella typhi* ATCC.23594 &*Escherichia coli* ATCC.25922), Unicellular Fungi (*Candida albicans* ATCC.10231) and Multicellular Fungi (*Aspergillus brasiliensis* ATCC.16404) using agar disk diffusion method (Kirby-Bauer Method). In this technique, 6.0 mm diameter discs were impregnated with different concentrations of nanoparticles (0.1, 0.5, 1, 2mg/l) followed by sterilization [24].

Mueller Hinton agar plates were used for prokaryotic and unicellular fungi while multicellular fungi were inoculated on Czapek Dox agar as per CLSI guidelines. The plates were incubated at 35 ± 2 □ for 16-18hrs (bacteria and unicellular fungi) and 28 ± 2 □ for 72hrs (multicellular fungi). Standard antimicrobial agents ampicillin (for Gram-negative bacteria, 10 mcg/disc), streptomycin (for Gram-positive bacteria, 10 mcg/disc), and amphotericin B (for unicellular and multicellular fungi, 100 units/disc) were used as controls. All assays were performed in triplicates. The diameter of inhibition zones around the discs was measured (mm) and the results were recorded [25].

Photo-oxidative dye degradation:

10 mg of prepared Cu nanoparticle was added to the 200 mL of different concentrations of Red M8B and Reactive green dye solution (100-600µg/mL) to the suspension in a 250 mL beaker. The initial concentration of dyes was determined by taking a little amount of suspension in a semi-micro test tube just after mixing. Then the subsequent mixture was allowed to remain underneath the sunlight for 6h [26]. After that, suspensions were collected in test tubes for 6hrs and centrifuged at a constant speed for 20 minutes to settle the degraded matter. The absorbance of these centrifugates was measured at λ_{max} of Red M8B and Reactive green dye using deionized water as a reference. The pH of deionized water was kept the same as the pH of the suspension. The degradation efficiency (%) was determined by the following Equation.

$$\text{Degradation Efficiency (\%)} = \left(\frac{C_0 - C_t}{C_0}\right) \text{X } 100$$

Where, C_0 is the initial concentration and C_t is the final dye concentration with time t in the aqueous phase, respectively [27].

Fig. 1. Collection of soil samples from different locations of mangroves a) Gorai Beach, b) Godrej Mangroves, and c) and d) Vikhroli Mangroves.

The concentration at which the highest degradation of dye is observed was used for a time-dependent degradation assay. The 200 mL of dye solution of concentration at which the highest degradation was observed was taken in a 250 mL flask and 10mg of CuNPs was added to it. After that at different time intervals (0-6hrs) samples were collected and centrifuged at a constant speed for 20 minutes. . The concentration of remaining dye after the photocatalytic experiment was determined by measuring the absorbance of dye at λ_{max} of Red M8B and Reactive green dye using deionized water as a reference [26].

Antibiofilm Activity

Prevention of biofilm formation by CuNPs was confirmed by microscopic technique. Briefly, the glass slide was dipped in CuNPs solution and dried in the oven after that this slide along with the glass slide without CuNPs (Control) was placed in a tank filled with seawater collected from Indira dock located in Mumbai (18.9416° N, 72.8409° E) for 48hrs at room temperature. After incubation, the slides were subjected to Crystal violet staining stained glass slides and were inspected by light microscopy at magnifications 45X and 100X [28].

RESULTS AND DISCUSSION

Collection of soil sample

Eight different soil samples were collected from three different mangrove sites located in Mumbai (**Fig 1.**). The soil samples collected at 5-15 cm depth helped to get a maximum number of aerobic *Actinomycetes*. The pH of the fresh soil samples was ranging from 7.5 to 8.2. Air drying the soil samples for a week and then treating them at 45˚C for 1hr helped to eliminate the vegetative bacteria and fungi.

Isolation of Actinomycetes

This soil was then serially diluted and a spread plate was performed on AIA, SNA, and SCA. The plates were incubated for 5-7 days and the colonies were distinguished based on colony characteristics such as tough, leathery, mucoid colonies which are partially submerged in the agar (**Fig 2.**). The suspected *Actinomycetes* colonies were purified using the respective media from which it was isolated. A total of 15 different *Actinomycetes* isolates were obtained from soil samples and studied in the present investigation. Well-grown isolates were maintained on Glycerol asparagine agar (GAA) medium supplemented with antifungal griseofulvin (50µg/mL).

Screening of Actinomycetes for metal tolerance

The *Actinomycetes* isolates were assessed for the tolerance of metal at different concentrations i.e. 10^{-9} M, 10^{-7} M, 10^{-5} M, 10^{-3} M, and 10^{-1} M of $AgNO_3$, $MnSO_4$, $CuSO_4$, and $ZnSO_4$. It was found

Fig. 2. Primary isolation of actinomycetes from soil a) on AIA, b) on SCA

Table 1. Growth at different salt concentrations. (+ Resistant, - Sensitive)

Sr. No.	Metal Salts	Salt Concentration	Isolates								
			GRC2	GRC4	GRN2	DBC4	GRN1	VKN3	VKN4	DBC3	GRC3
1.	$AgNO_3$	10^{-9} M	+	+	+	+	+	+	+	+	+
		10^{-7} M	-	-	-	-	-	+	+	+	+
		10^{-5} M	-	-	-	-	-	+	+	+	+
		10^{-3} M	-	-	-	-	-	-	-	-	-
		10^{-1} M	-	-	-	-	-	-	-	-	-
2.	$CuSO_4$	10^{-9} M	+	+	+	+	+	+	+	+	+
		10^{-7} M	-	-	-	-	+	+	+	+	+
		10^{-5} M	-	-	-	-	-	+	+	+	+
		10^{-3} M	-	-	-	-	-	-	-	-	-
		10^{-1} M	-	-	-	-	-	-	-	-	-
3.	$MnSO_4$	10^{-9} M	+	+	+	+	+	+	+	+	+
		10^{-7} M	-	-	-	-	-	+	+	+	+
		10^{-5} M	-	-	-	-	-	+	+	+	+
		10^{-3} M	-	-	-	-	-	-	-	-	-
		10^{-1} M	-	-	-	-	-	-	-	-	-
4.	$ZnSO_4$	10^{-9} M	+	+	+	+	+	+	+	+	+
		10^{-7} M	-	-	-	-	+	+	+	+	+
		10^{-5} M	-	-	-	-	-	+	+	+	+
		10^{-3} M	-	-	-	-	-	-	-	-	-
		10^{-1} M	-	-	-	-	-	-	-	-	-

that out of 15 isolates only 3 isolates were able to tolerate the highest metal salt concentration i.e. 10^{-1} M. All isolates were able to grow at 10^{-7} except GRC2, GRC4, GRN2, and DBC4. These isolates were able to tolerate a minimum of 10^{-9} metal salts concentration. Isolate GRN1 was an exception as this isolate was unable to tolerate 10^{-7} concentrations of $AgNO_3$ and $MnSO_4$ but was able to tolerate the same concentration of $CuSO_4$, and $ZnSO_4$. Isolates VKN3, VKN4, DBC3, and GRC3 were able to tolerate all metal salts till 10^{-5} M concentration but were sensitive to higher concentrations i.e. 10^{-3} M & 10^{-1} M (Table 1.).

Isolates DBC1 was able to tolerate 10^{-5}M concentration of $CuSO_4$ and $MnSO_4$ but were able to tolerate only 10^{-7} M concentration of $AgNO_3$ and

Table 2. Growth at different salt concentrations. (+ Resistant, - Sensitive)

Sr No.	Metal salts	Salt Concentration	Isolates					
			GRC1	GRN3	DBC1	DBC2	VKN1	VKN2
1	$AgNO_3$	10^{-9} M	+	+	+	+	+	+
		10^{-7} M	+	+	+	+	+	+
		10^{-5} M	+	-	-	+	+	+
		10^{-3} M	+	-	-	+	+	-
		10^{-1} M	+	-	-	+	+	-
2	$CuSO_4$	10^{-9} M	+	+	+	+	+	+
		10^{-7} M	+	+	+	+	+	+
		10^{-5} M	+	-	+	+	+	+
		10^{-3} M	+	-	-	+	+	-
		10^{-1} M	+	-	-	+	+	-
3	$MnSO_4$	10^{-9} M	+	+	+	+	+	+
		10^{-7} M	+	+	+	+	+	+
		10^{-5} M	+	+	+	+	+	+
		10^{-3} M	+	-	-	+	+	+
		10^{-1} M	+	-	-	+	+	+
4	$ZnSO_4$	10^{-9} M	+	+	+	+	+	+
		10^{-7} M	+	+	+	+	+	+
		10^{-5} M	+	+	-	+	+	+
		10^{-3} M	+	-	-	+	+	-
		10^{-1} M	+	-	-	+	+	-

$ZnSO_4$. Similarly isolate GRN3 was able to tolerate 10^{-5} M concentration of $ZnSO_4$ and $MnSO_4$ but was unable to grow at concentrations 10^{-5} M, 10^{-3} M, and 10^{-1} M of $AgNO_3$ and $CuSO_4$. Although isolates DBC2, GRC1, and VKN1 were able to tolerate even 10^{-1} M concentration of all metal salts making them excellent candidates for nanoparticle biosynthesis (Table 2.).

The *Actinobacteria* have an inherent metal tolerance property due to their metal detoxification mechanisms. They can alter heavy metal toxicity by using various metal-independent mechanisms such as reduction of cellular sensitivity, intracellular metal sequestration, siderophore-metal complexation, and exclusion through permeability barriers. It is already known that few *Streptomyces* sp. can tolerate heavy metals like *Streptomyces albulus* PD-1 [29], *Streptomyces lunalinharesii* [30], *Streptomyces fradiae* [31], and *Streptomyces zinciresistens* [32] which were reported to be tolerant to heavy metals like Zn (II), Cd (II), Cu (II), Cr (VI), Ni (II), and Pb (II).

Bio-fabrication of copper nanoparticles

Actinomycetes isolates exhibiting metal resistance were inoculated in a 250 mL flask containing Tryptone Yeast Extract Broth and incubated, after incubation, the CFS was obtained. When the CFS was added to 10mM CuSO4 solution color change was observed from colorless to dark brown color which indicates the synthesis of CuNPs. Although the CFS of three isolates that were metal tolerant (DBC2, GRC1, and VKN1) were used for the fabrication of CuNPs only one isolate i.e. GRC1 was able to synthesize CuNPs which was evident by the change in color from blue to brown (**Fig 3.**). The color change was due to the size-dependent property of nanoparticles which is a property of quantum confinement that affects the optical property of the nanoparticles. This reduced aqueous component was further used for characterization purposes.

Many researchers have reported the biosynthesis of copper nanoparticles by using CFS as well as *Actinomycetes* biomass. Recently microorganisms-mediated fabrication of CuNPs was achieved by using *Agaricus bisporus* [33], *Streptomyces* MHM38 [34], *Lactobacillus caseisubsp. casei* [35], *Pseudomonas fluorescens, Trichodermaatroviride*, and *Streptomyces griseus* [36]. Hassan et al. [37] in his study synthesized CuNPs by using endophytic *Streptomyces capillispiralis* Ca-1 in which the color change from light blue to greenish brown color was reported. In a study by Fouda et al., [38] he used endophytic *Actinomycetes* isolated from the medicinal plant *Oxalis corniculata* L. to synthesize CuNPs. The isolates were identified as *Streptomyces zaomyceticus* Oc-5 and *Streptomyces pseudogriseolus*

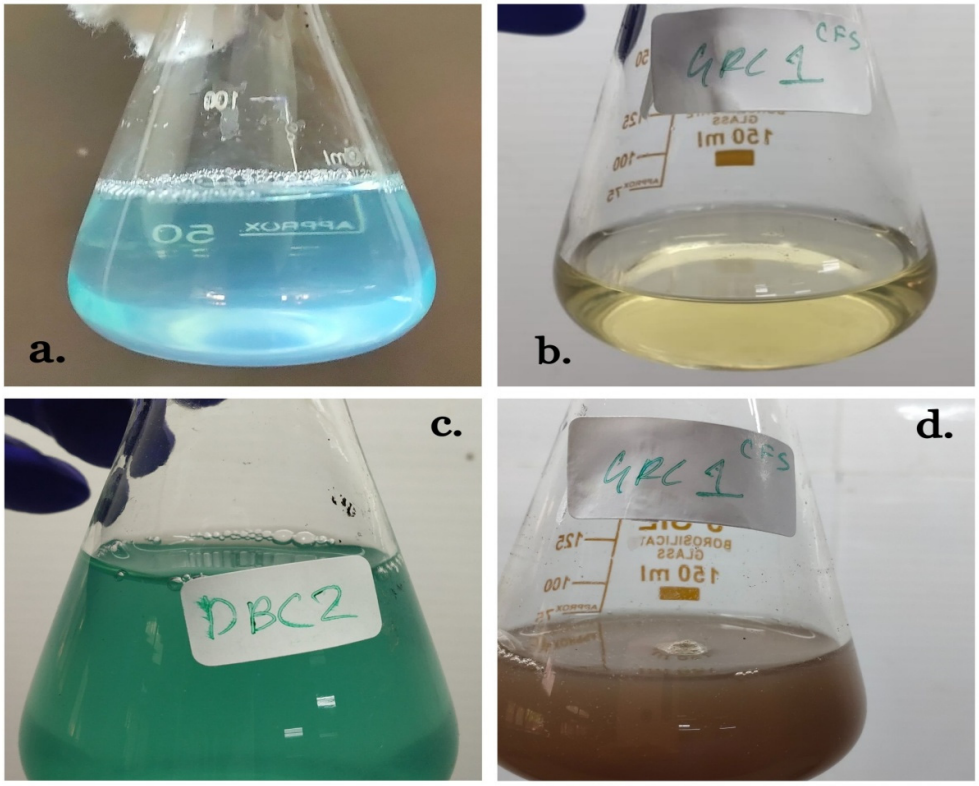

Fig. 3. Bio fabrication of CuNPs a) 10mM CuSO4, b) CFS, c) CuSO4 + CFS (before heat treatment), d) CuSO4 + CFS (after heat treatment).

Acv-11 and the synthesis was visible by a change in color from light blue to brown.

Identification of Actinomycetes

As isolate GRC1 was the only metal-tolerant *Actinomycete* strain that was able to synthesize CuNPs thus the identification of isolate GRC1 was done as per Bergey's Manual of Systematic Bacteriology Volume 5. *Actinobacteria* and fundamentals mentioned by McCarthy and Williams (1990) for preliminary identification of *Actinomycetes*. The following properties of *Actinomycetes* were used for the identification of the isolate GRC1.

Colony characteristics

Isolate GRC1 exhibited white color mycelia and had yellowish-brown pigmentation when observed from the back of the plate (**Fig. 4.**).

Pigmentation

On glycerol asparagine agar, no discussible pigmentation was observed, colony mycelia pigmentation was white in color and the reverse side of the colony exhibited yellowish-brown pigment.

Microscopic characteristics

The microscopic observations were studied using the coverslip culture technique the isolate GRC1 exhibited spore chain morphology (**Fig. 5.**). In the study by Rathore et al., [39] the morphology characters of isolated *Actinomycetes* strains were performed for identification. The microscopic examination revealed long thread-like structures, fragmentation of the mycelia, and violet-colored cell morphology. Similarly, Tesche et al., [40] reported heterogeneous mycelial morphology when observed under a microscope. The microscopical examination of *Actinomycetes* cell morphology was also explored by Singh and Gohel, [41] for the identification of *Actinomycetes*.

Biochemical Characteristics

The isolate GRC1 was able to utilize glucose, fructose, maltose, and inositol which was evident

Fig. 4. Isolate GRC1 exhibiting white mycelia.

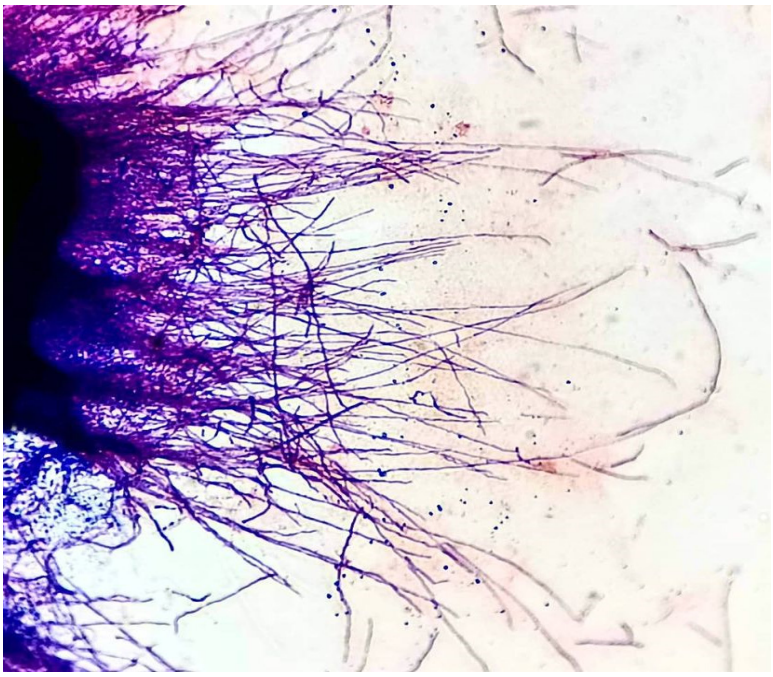

Fig. 5. Spore chain morphology of GRC1 isolate under microscope

by the growth observed in the tubes. But isolate GRC1 exhibited no growth in sucrose, mannitol, galactose, rhamnose, raffinose, arabinose, cellulose, and xylose as there was no growth observed in tubes containing these sugars (Table 3.). Isolate GRC1 when inoculated in peptone nitrate broth with a lead acetate strip and incubated exhibited no change of color in the lead acetate strip indicating that this isolate is unable to produce H_2S. After the addition of hydrogen peroxide on the slide with the culture of GRC1 evolution of air bubbles was not observed indicating the absence of catalase enzyme in the GRC1 isolate.

The isolate GRC1 was found to be positive for gelatinase, caseinase, amylase, cellulose, urease, and lipase but was negative for only lecithinase.

Table 3. Utilization of different carbon source (+ Growth, - No growth)

Carbon Substrate	Growth
Sucrose	-
Glucose	+
Fructose	+
Maltose	+
Mannitol	-
Galactose	-
Rhamnose	-
Raffinose	-
Arabinose	-
Cellulose	-
Xylose	-
Inositol	+

Table 4. Enzyme activity of GRC1 (+ Positive activity, - Negative activity)

Tests	Enzyme Activity
Gelatinase	+
Caseinase	+
Amylase	+
Cellulase	+
Lacithinase	-
Urease	+
Lipase	+

It was also able to hydrolyze starch all the details are summarized in Table 4. In these past years, many researchers in their early investigation have reported that soil and mangrove water sediment areas possess enzymatically active *Actinomycetes*. As per the Bergey's Manual of Systematic Bacteriology Volume 5. (*Actinobacteria*) and fundamentals mentioned by McCarthy and Williams (1990) the isolate GRC1 was identified to be Streptomyces sp. This isolate was further characterized by Vitek MS and it was identified as *Streptomyces verticillus*.

Characterization of CuNPs:

UV-VISIBLE SPECTROSCOPY: UV-visible absorption spectra of a methanol solution containing a colloidal suspension of Cu NPs. Due to the simultaneous vibration of the electrons of metal nanoparticles in resonance with a light wave, the surface plasmon resonance (SPR) absorption band is visible at 576 nm. The wide size distribution of copper nanoparticles is what causes the broad absorption band that has been seen. The surface-plasmon band is significantly influenced by the solvents, reducing agents, and nanoparticle size and shape used in the synthesis. (Fig. 6).

TRANSMISSION ELECTRON MICROSCOPY: In (Fig.7), a study conducted using a high-resolution transmission electron microscope, the behavior of CuNPs was observed. The particle size of the CuNPs was localized and assigned as a nano size. Cu-NPs are produced biologically as a result of electrostatic interactions and molecular bonds between the bio-organic capping molecules. The TEM investigation showed that nanocrystalline Cu-NPs was formed, with the majority of them adopting spherical morphologies and aggregating into tiny aggregates with average diameters of about 42 nm (S.D.) and sizes ranging from 13 to 35 nm.

FTIR: The molecules of the physiologically active compounds found in the Cu NPs powder were identified using FTIR spectra analysis. This investigation (Fig.8), is used to recognize the bio-molecules which account for the reduction, capping, and stabilization of the fabricated Cu-NPs. The FTIR spectrum peak at 3330.90 cm^{-1} indicates the O–H stretching of alcohols and phenols, the peak at 2972.95 cm^{-1} represents Methyl C–H stretching (asymmetrical), the peak at 2882.59 cm^{-1} represents Methyl C–H stretching (symmetrical), peak at 1465.11 cm^{-1} denotes the vibrations of bending modes, peak at 2368.78 cm^{-1} represents N–H band of primary amines related components, peak at 2281.85 cm^{-1} indicates the C=C Medial Alkyne groups, peak at 2124.805 cm^{-1} indicates the

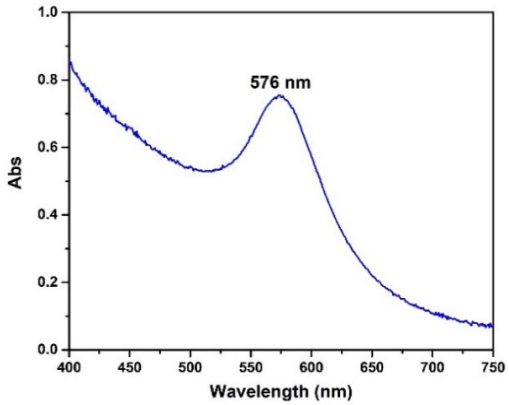

Fig. 6. UV GRAPH

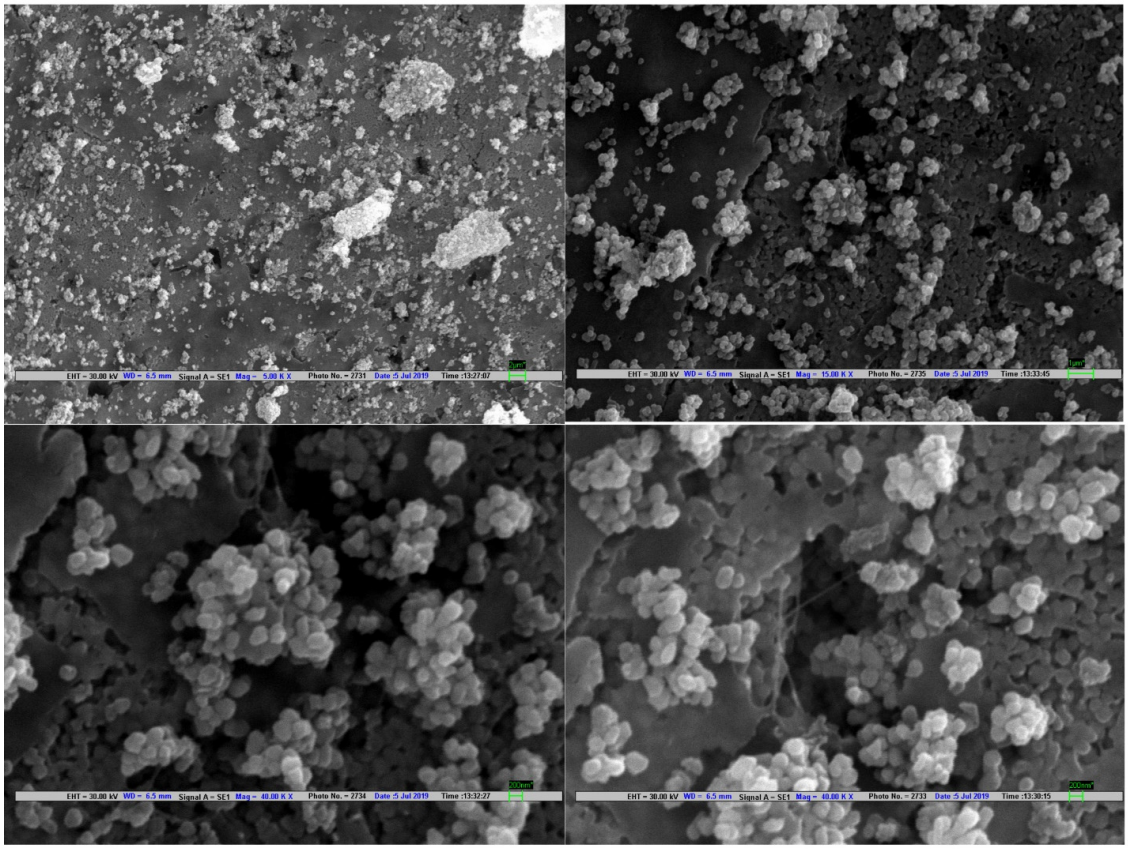

Fig. 7. TEM

C=C Terminal Alkyne groups, peaks at 2091.79 and 1921.772 cm^{-1} represents copper carbonyls, peak at 1734.07 cm^{-1} denotes Alkyl Carbonate, peak at 1379.67 cm^{-1} corresponds to the Nitrate ion, peak at 1044.503 cm^{-1} indicates the Carbonate ion, while the last corresponding peak at 802.112 cm^{-1} shows the Aliphatic Chloro-compound C–Cl stretching. Thus, FTIR results conclude that the proteins and acids surrounding the Cu-NPs are inducing the reduction of copper ions into nanoparticles.

Applications of copper nanoparticles

Antimicrobial Activity

The zone of inhibition in mm exhibited by

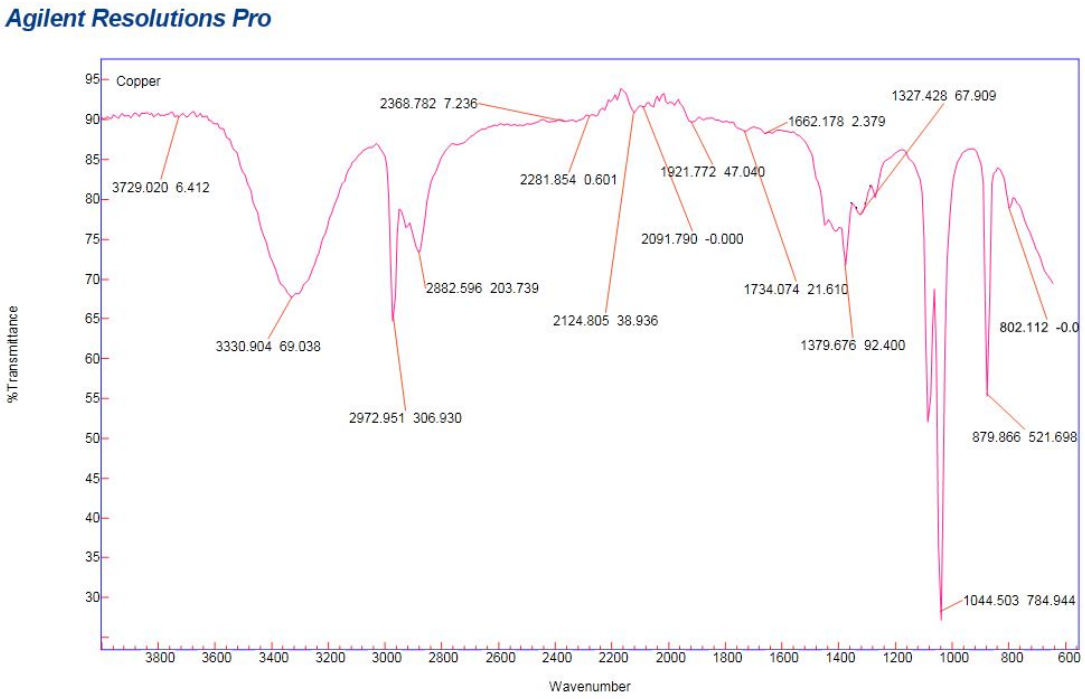

Fig. 8. FTIR

Fig. 9A. & Fig. 9B. Antimicrobial sensitivity of *Staphylococcus aureus*

D/W was 0 for all the test organisms and the zone of inhibition exhibited by $CuSO_4$ solution against *Staphylococcus aureus* ATCC.25923 (**Fig. 9A.**), *Streptococcus pyogenes* ATCC.25663 (**Fig. 10A**.), *Shigella sp.* ATCC.23354 (**Fig. 11A**.), *Escherichia coli* ATCC.25922 (**Fig. 12A**.), *Candida albicans* ATCC.10231, and *Aspergillus brasiliensis* ATCC.16404 were 7mm, 0mm, 14mm, 18mm, 0mm, and 0mm respectively.

The zone of inhibition observed by Amphotericin B for *Aspergillus brasiliensis* ATCC.16404 and *Candida albicans* ATCC.10231 was 10mm and 19mm respectively. Similarly zone of inhibition by Ampicillin for *Shigella sp.* ATCC.23354 and *Escherichia coli* ATCC.25922 were 10mm, and 24mm respectively. The zone of inhibition obtained by Streptomycin against *Staphylococcus aureus* ATCC.25923 and *Streptococcus pyogenes* ATCC.25663 was 25mm and 20mm respectively. Finally the zone of inhibition obtained by

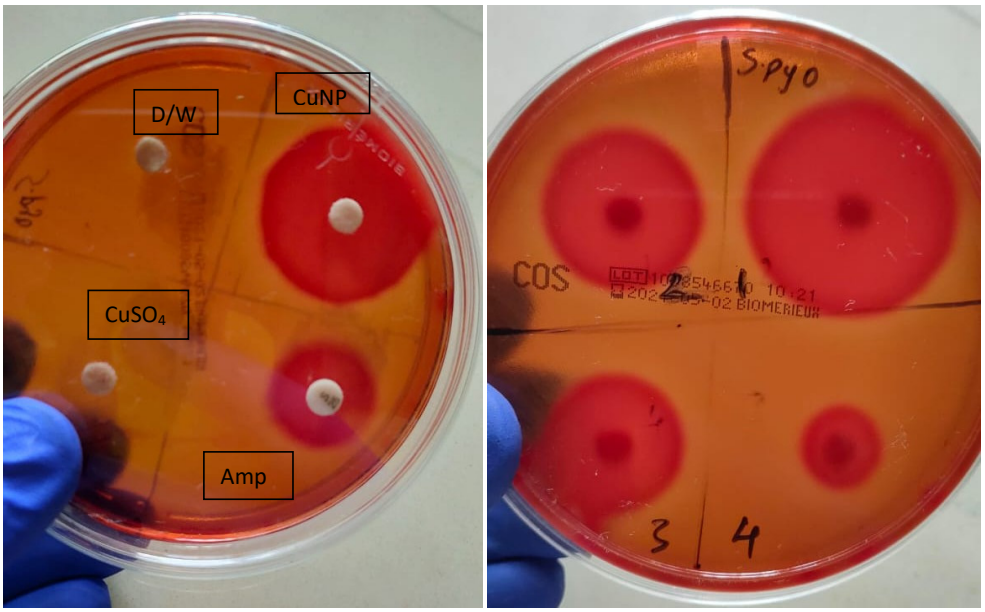

Fig. 10A. & Fig. 10B. Antimicrobial sensitivity of *Streptococcus pyogenes*

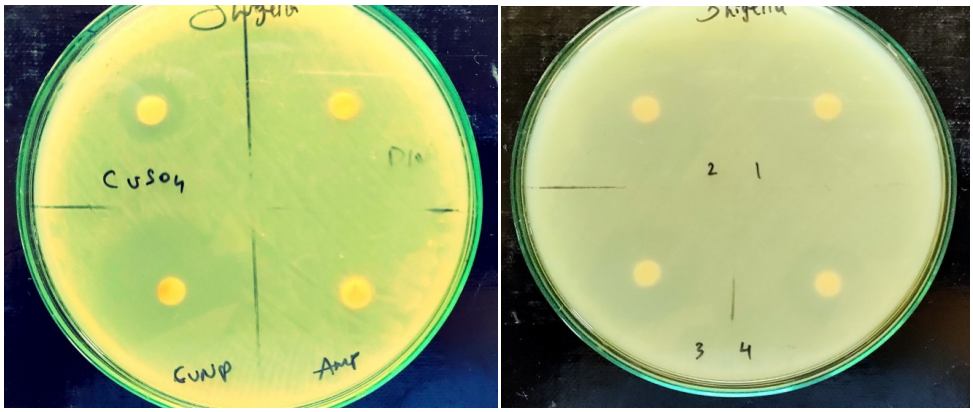

Fig. 11A. & Fig. 11B. Antimicrobial sensitivity of *Shigella sp.*

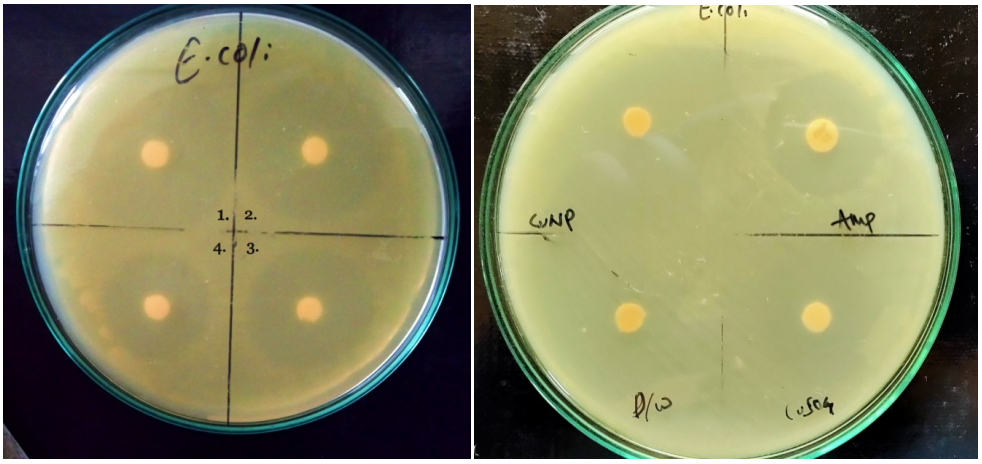

Fig. 12A. & Fig. 12B. Antimicrobial sensitivity of *Escherichia coli*

Table 5. Antimicrobial activity of CuNPs

Sr No.	Test Microorganisms	Zone of inhibition (mm)					
		D/W	$CuSO_4$	CuNPs	AmB	Amp	Stm
1.	*Staphylococcus aureus* ATCC.25923	**O**	**7**	**27**	-	-	**25**
2.	*Streptococcus pyogenes* ATCC.25663	**0**	**0**	**30**	-	-	**20**
3.	*Shigella sp.* ATCC.23354	**0**	**14**	**35**	**10**	-	-
4.	*Escherichia coli* ATCC.25922	**0**	**18**	**35**	-	**24**	-
5.	*Candida albicans* ATCC.10231	**0**	**0**	**24**	**19**	-	-
6.	*Aspergillusbrasiliensis* ATCC.16404	**0**	**0**	**15**	**10**	-	-

Table 6. Antimicrobial activity by different CuNPs concentrations

Sr No.	Test Microorganisms	Zone of inhibition (mm)			
		0.1mg/l	0.5mg/l	1mg/l	2mg/l
1.	*Staphylococcus aureus* ATCC.25923	**8**	**14**	**20**	**27**
2.	*Streptococcus pyogenes* ATCC.25663	**12**	**19**	**24**	**30**
3.	*Shigella sp.* ATCC.23354	**16**	**20**	**26**	**31**
4.	*Escherichia coli* ATCC.25922	**10**	**16**	**22**	**35**
5.	*Candida albicans* ATCC.10231	**7**	**11**	**15**	**24**
6.	*Aspergillusbrasiliensis* ATCC.16404	**0**	**4**	**10**	**15**

biosynthesized CuNPs for *Staphylococcus aureus* ATCC.25923, *Streptococcus pyogenes* ATCC.25663, *Shigella sp.* ATCC.23354, *Escherichia coli* ATCC.25922, *Candida albicans* ATCC.10231, and *Aspergillus brasiliensis* ATCC.16404 were found to be 27mm, 30mm, 30mm, 35mm, 24mm, and 15mm respectively. The zone of inhibition was significantly great by biosynthesized CuNPs when compared with standard antibiotics and $CuSO_4$ (Table 5.).

After exploring the antimicrobial activity of synthesized CuNPs the efficiency of CuNPs with different concentrations (0.1, 0.5, 1, 2 mg/L) was accessed. The zone diameter observed by 2 mg/L CuNPs concentration discs for *Staphylococcus aureus* ATCC.25923 (Fig. 9B.), *Streptococcus pyogenes* ATCC.25663 (Fig.10B.), *Shigella* sp. ATCC.23354 (Fig. 11B.), *Escherichia coli* ATCC.25922 (Fig.12B.), *Candida albicans*ATCC.10231, and *Aspergillus brasiliensis* ATCC.16404 were 27mm, 30mm, 31mm, 35mm, 24mm, and 15mm respectively, and for 1 mg/L was 20mm, 24mm, 26mm, 22mm, 15mm, and 10mm respectively. Similarly the concentration of 0.5 mg/L for *Staphylococcus aureus* ATCC.25923, *Streptococcus pyogenes* ATCC.25663, *Shigella* sp. ATCC.23354, *Escherichia coli* ATCC.25922, *Candida albicans* ATCC.10231, and *Aspergillus brasiliensis* ATCC.16404 were 14mm, 19mm, 20mm, 16mm, 11mm, and 4mm respectively, and by 0.5 mg/L was 8mm, 12mm, 16mm, 10mm, 7mm, and 0mm respectively (Table 6.). Metallic copper nanoparticles (NPCu) and nanoparticles of copper oxides (NPCuO) have been reported as active agents against different pathogens of infections associated with health care. Hassan et al., [42] reported promising antifungal activities at different concentrations (5, 10, 15, and 20 mM) of CuNPs. The maximum inhibition of 57.14, 63.81, 42.61, and 58.05% against *Alternaria* spp., *Aspergillusniger, Fusarium* spp., and *Pythium*spp were recorded at a concentration of 20 mM by Kumar et al., respectively [43]. the investigation of the Hybrid cellulose nanocomposite films (HCNFs) with Copper nanoparticles and reported that the hybrid nanocomposites exhibited better antibacterial properties against *E. coli, P. aeruginosa* (Gram Negative), and *S. aureus, B. licheniformis* (Gram Positive). In a recent study by Benassai et al., [44] he synthesized copper nanoparticles (Cu-NPs) using aqueous extracts of *Vacciniummyrtillus L.* and *Vacciniumuliginosum L.* subsp. *gaultherioides.* He reported that the antimicrobial activity of Cu-NPs, especially those derived from bilberry waste residues, appeared to be higher for both Gram-negative (*E. coli ATCC29213*) and Gram-positive bacteria (*S. aureus ATCC35218*), and fungi (*S. cerevisiae, C. Albicans*), compared to the ones of its single components (cupric salts and berry extracts).

Photo-oxidative dye degradation

In this study, Photo-oxidative degradation

of Red M8B and Reactive green dyes were investigated under direct sunlight at room temperature with continuous stirring at constant pH. The degradation of Red M8B and Reactive green dyes were measured at an absorbance at 450 and 630 nm as maximum absorption was observed at these wavelengths, respectively (**Fig. 13A.**). Different concentrations of Red M8B and Reactive green dye solution (100-600µg/mL) was treated with CuNPs (**Fig.14**.) the calculated degradation efficiency of Red M8B and Reactive green at 100µg/mL were 61.84% and 87.46% respectively (**Fig. 15.**). This is a quite good degradation efficiency as both Red M8B and Reactive green dye has a very complex molecular structure and high molecular weight of 1338.062 g/mol and 1418.93000 g/mol respectively. A time-dependent degradation assay was carried out using 100µg/mL concentration of Red M8B and Reactive green (**Fig. 16.**). After 5hrs of incubation, almost complete degradation of Red M8B and Reactive green was observed. The calculated degradation efficiency after 5hrs of incubation was 59.67% and 96.26% for Red M8B and Reactive green respectively (**Fig. 17.**).

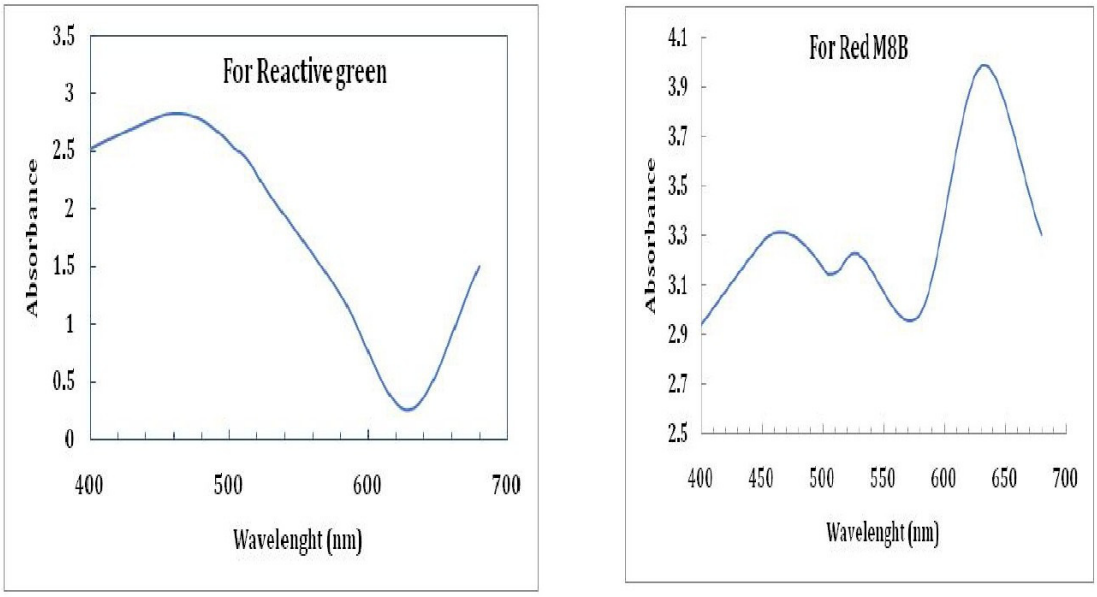

Fig. 13. Absorption Maxima of Red M8B and Reactive Green Dye

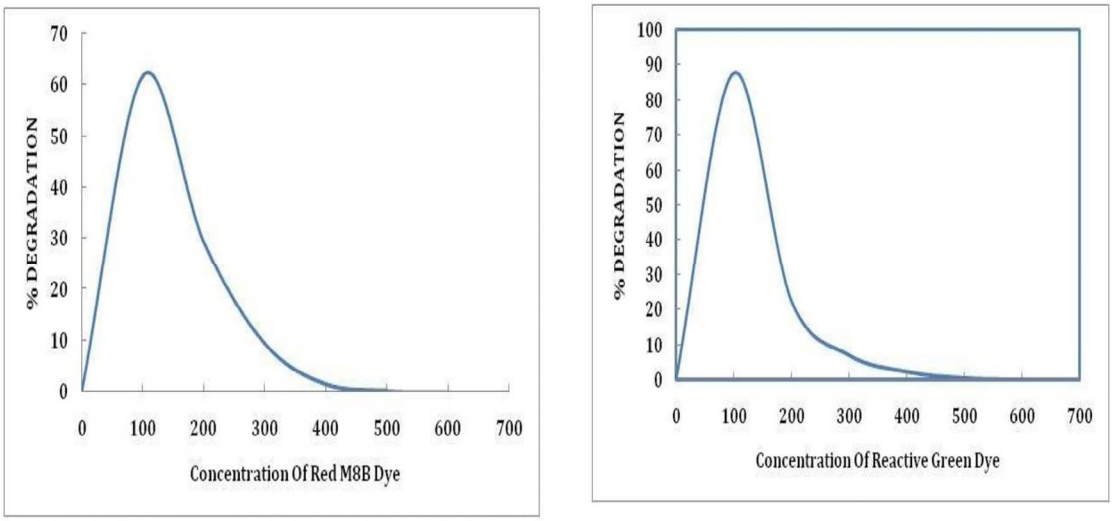

Fig. 14. Percent Degradation of Red M8B and Reactive Green Dye at different concentrations

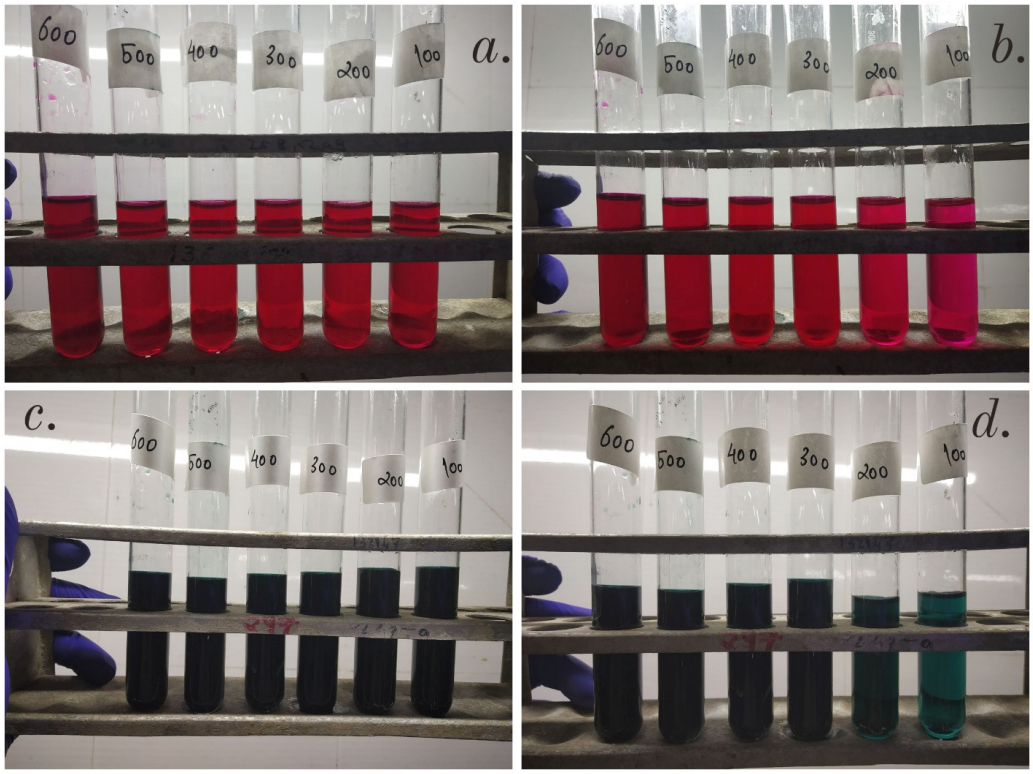

Fig. 15. Dye degradation at different concentration a) Red M8B before treatment with CuNPs, b) Red M8B after treatment with CuNPs, c) Reactive Green before treatment with CuNPs,d) Reactive Green after treatment with CuNPs.

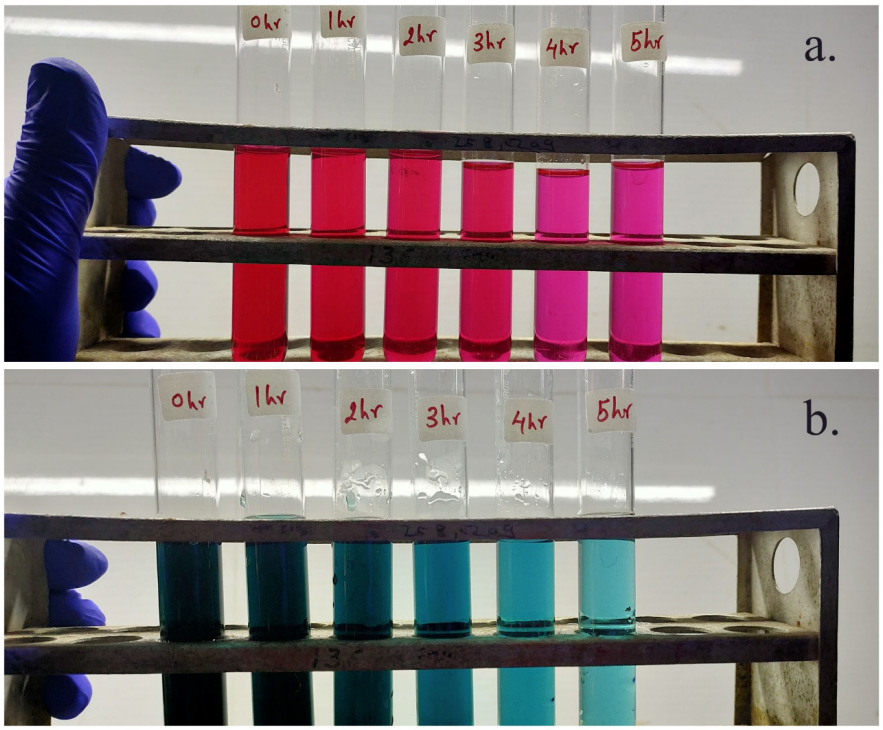

Fig. 16. Dye degradation at different Time Intervals a) Red M8B, b) Reactive Green

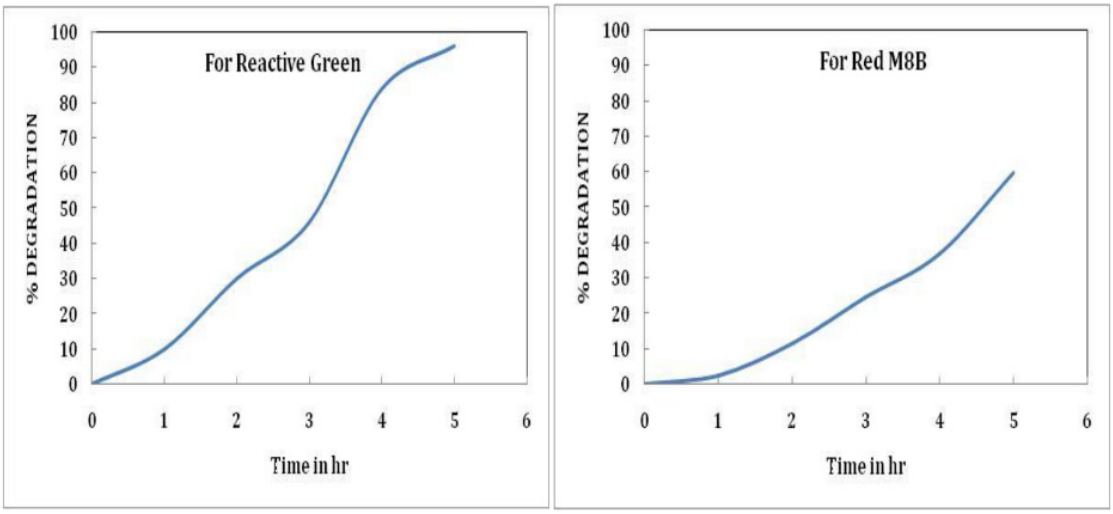

Fig. 17. Percent degradation of Red M8B and Reactive Green Dye at different Time Intervals

Sharma and Dutta [45] reported that the hydroxy radicals were dominant reactive oxygen species that contributed to degradation when using CuONPs. These authors performed the scavenger experiment in which Isopropyl alcohol was used as a scavenger for hydroxy radicals. Thus, their study provided a suitable justification for active species-based photocatalytic degradation of dyes when using CuONPs. In this work, control experiments (both in the presence and absence of CuNPs) were carried out in the dark to nullify any possibility of dye self-degradation, dye adsorption, and catalytic activity of NPs in dark. After completion of the experiment, negligible degradation for dye in the absence of CuNPs was observed. Likewise, under dark conditions, CuNPs exhibited only an insignificant effect on the degradation of dye. Thus, it was concluded that the dyes were not significantly adsorbed/ degraded in dark conditions. In addition, dye degradation experiments under direct sunlight in the absence of CuNPs showed negligible dye degradation. In contrast, under direct sunlight with a catalyst both Red M8B and Reactive green were almost completely degraded. These experiments demonstrated that dye degradation was driven by a photocatalytic process.

In a study by Raheem et al., [46] photocatalytic degradation of Reactive green was reported. He observed that as the concentration of reactant increased the degradation efficiency increased until the concentration reached 0.12gm/mL after that it was constant. Salar et al., [47] also reported maximum degradation of 62.27% for Red M8B dye. Similarly, Thakare [48] has reported degradation of Red M8B and Reactive green with an efficiency of 30% and 50% respectively. This indicates that the complex structure and high molecular weight of the dye play a crucial role in degradation also very little work has been done on these two dyes.

Antibiofilm Activity

Prevention of biofilm formation by CuNPs was confirmed by microscopic technique and significant inhibition of biofilm was observed (**Fig. 18.**). This property of biofilm inhibition by biosynthesized CuNPs can be used to inhibit marine biofouling. As marine biofilms easily colonize man-made surfaces, accelerating corrosion, and biofouling [49], and may even influence the buoyance of polyethylene plastic [50].

Summary and Conclusion

Bionanotechnology is a better forthcoming opportunity for nanomaterial science. Metal NPs often exhibit activity different from that of the corresponding bulk materials because of their different sizes and shapes, which give rise to distinctive quantum properties. Since copper resembles the properties of gold and silver according to the periodic table it can be used as an alternative cheap nanoparticle to the expensive gold and silver nanoparticles.

In the present study green, eco-friendly, simple, and inexpensive techniques were used for

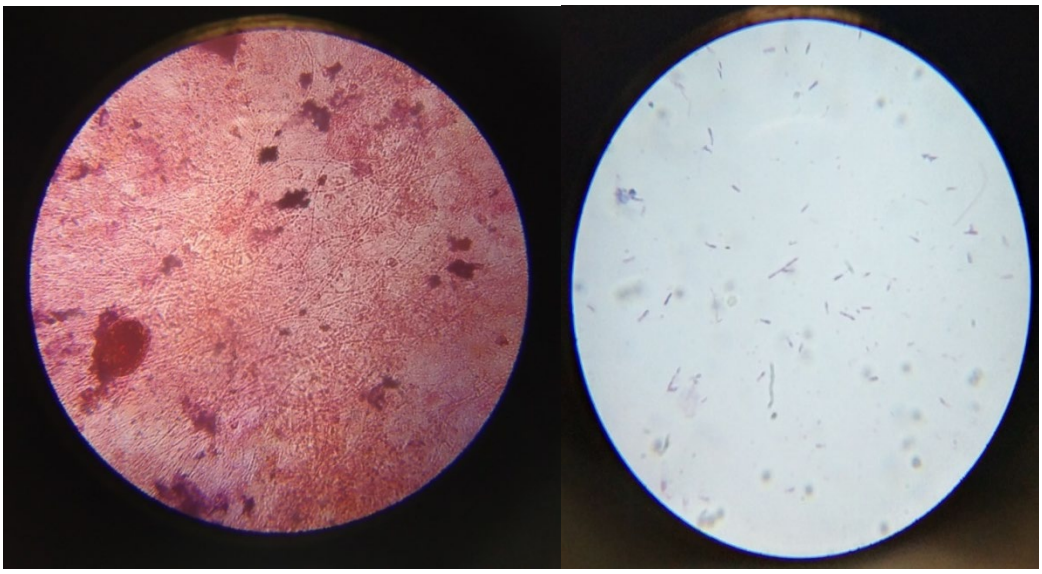

Fig. 18. Biofilm Slide without CuNPs and with CUNPs

the biosynthesis of copper nanoparticles using mangrove *Actinomycetes* isolated from Mumbai, Maharashtra. Eight different soil samples were collected from three different mangrove sites located in Mumbai. A total of 15 different *Actinomycetes* isolates were obtained from soil samples and studied in the present investigation and were screened for metal tolerance. The *Actinomycetes* isolates were assessed for the tolerance of metal at different concentrations i.e. 10^{-9} M, 10^{-7} M, 10^{-5} M, 10^{-3} M, and 10^{-1} M of $AgNO_3$, $MnSO_4$, $CuSO_4$, and $ZnSO_4$. It was found that out of 15 isolates, only 3 isolates were able to tolerate the highest metal salt concentration i.e. 10^{-1}M.

The present study was focused to examine the potential of metal-tolerant *Actinomycetes* for the synthesis of CuNPs and it was found that only one of the three metal-tolerant isolates was able to synthesize CuNPs when its CFS was treated with CuSO4. The color change from light blue to brown color indicates the synthesis of CuNPs which was further investigated with various characterizations such as UV-Vis spectroscopy, FTIR, and XRD. As isolate GRC1 was the only metal-tolerant *Actinomycetes* strain that was able to synthesize CuNPs thus the identification of isolate GRC1 was done as per Bergey's Manual of Systematic Bacteriology Volume 5. *Actinobacteria* and fundamentals were mentioned by McCarthy and Williams (1990) for preliminary identification of *Actinomycetes* and were identified as *Streptomyces* sp. This isolate was further characterized by Vitek MS and it was identified as *Streptomyces verticillus*.

The zone of inhibition obtained by biosynthesized CuNPs for *Staphylococcus aureus* ATCC.25923, *Streptococcus pyogenes* ATCC.25663, *Shigella* sp. ATCC.23354, *Escherichia coli* ATCC.25922, *Candida albicans* ATCC.10231, and *Aspergillus brasiliensis* ATCC.16404 were found to be 27mm, 30mm, 30mm, 35mm, 24mm, and 15mm respectively. The zone of inhibition was significantly great by biosynthesized CuNPs when compared with standard antibiotics and CuSO4.

From the result, it can be concluded that the effectiveness of bio-fabricated CuNPs was as high as a strong antimicrobial agent which can be used in the food industry, cosmetics, and medicine also the biogenic CuNPs were found to inhibit the growth and multiplication of the tested bacteria at a very low total concentration of CuNPs. Biofabricated CuNPs showed very high photocatalytic activity and were found to be used in the degradation of dyes like Reactive green, and Red M8B under the influence of sunlight. The high photocatalytic activity of CuNPs against molecules of dye was due to the use of natural, and eco-friendly *Actinomycetes* CFS extract which reacts as a reducing agent for the synthesis of CuNPs and can be used in wastewater treatment plants.

Moreover, the recycling of biogenic CuNPs could be performed and used efficiently, thereby making the process cost-effective. Thus the mangrove *Actinomycetes* mediated bio fabrication of CuNPs should gain much attention because of their unique properties like antimicrobial, anticancer, catalytic activity, wound healing, and magnetic and optical properties.

CONFLICT OF INTEREST

The authors declare no conflict of interest.

REFERENCES

1. Guo, F., Yang, H., Liu, L., Han, Y., Al-Enizi, A. M., Nafady, A., ...& Ma, S. (2019). Hollow capsules of doped carbon incorporating metal@ metal sulfide and metal@ metal oxide core-shell nanoparticles derived from metal-organic framework composites for efficient oxygen electrocatalysis. Journal of Materials Chemistry A, 7(8), 3624-3631. https://doi.org/10.1039/C8TA11213D
2. Ghosh, M. K., Sahu, S., Gupta, I., &Ghorai, T. K. (2020). Green synthesis of copper nanoparticles from an extract of Jatrophacurcas leaves: characterization, optical properties, CT-DNA binding and photocatalytic activity. RSC Advances, 10, 22027-22035. https://doi.org/10.1039/D0RA03186K
3. Steckiewicz, K. P., & Inkielewicz-Stepniak, I. (2020). Modified nanoparticles as potential agents in bone diseases: cancer and implant-related complications. Nanomaterials, 10(4), 658. https://doi.org/10.3390/nano10040658
4. Gahlawat, G., & Choudhury, A. R. (2019). A review on the biosynthesis of metal and metal salt nanoparticles by microbes. RSC advances, 9(23), 12944-12967. https://doi.org/10.1039/C8RA10483B
5. Kumari, Suman, Tehri, N., Gahlaut, A., & Hooda, V. (2020). Actinomycetes mediated synthesis, characterization, and applications of metallic nanoparticles. Inorganic and Nano-Metal Chemistry, 1-10. https://doi.org/10.1080/24701556.2020.1835978
6. Khalil, A. M. A., Abdelaziz, A. M., Khaleil, M. M., & Hashem, A. H. (2021). Fungal endophytes from leaves of Avicennia marina growing in semi-arid environment as a promising source for bioactive compounds. Letters in Applied Microbiology, 72(3), 263-274. https://doi.org/10.1111/lam.13414
7. Khudur, L. S., Shahsavari, E., Webster, G. T., Nugegoda, D., & Ball, A. S. (2019). The impact of lead co-contamination on ecotoxicity and the bacterial community during the bioremediation of total petroleum hydrocarbon-contaminated soils. Environmental Pollution, 253, 939-948. https://doi.org/10.1016/j.envpol.2019.07.107
8. Daquioag, J. E. L., &Penuliar, G. M. (2021). Isolation of Actinomycetes with Cellulolytic and Antimicrobial Activities from Soils Collected from an Urban Green Space in the Philippines. International Journal of Microbiology, 2021, 1-14. https://doi.org/10.1155/2021/6699430
9. Sarika, K., Sampath, G., Govindarajan, R. K., Ameen, F., Alwakeel, S., Al Gwaiz, H. I., ...& Ravi, G. (2021). Antimicrobial and antifungal activity of soil Actinomycetes isolated from coal mine sites. Saudi Journal of Biological Sciences, 28(6), 3553-3558. https://doi.org/10.1016/j.sjbs.2021.03.029
10. Saba, Y., Muvva, V., &Munaganti, R. K. (2016). Isolation and Characterizationof Bioactive Streptomyces from Mangrove Ecosystem Ofmachilipatnam, Krishna District, Andhra Pradesh. Asian Journal of Pharmaceutical and Clinical Research, 9, 258. https://doi.org/10.22159/ajpcr.2016.v9s3.14913
11. Mali, G. V., & Gare, S. S. (2020). Optimization, Purification and Characterization of Tyrosinase from Novel Strain of Streptomyces Bikiniensis. Journal of Advanced Scientific Research, 11.
12. Aliero, Adamu & Ntulume, Ibrahim & Odda, John & Matilda, Angela. (2017). Production of novel antifungal compounds from Actinomycetes isolated from waste dump soil in Western Uganda. African Journal of Microbiology Research. 11. 1200-1210. https://doi.org/10.5897/AJMR2017.8588
13. Zhao, H., Maruthupandy, M., Al-mekhlafi, F. A., Chackaravarthi, G., Ramachandran, G., & Chelliah, C. K. (2022). Biological synthesis of copper oxide nanoparticles using marine endophytic Actinomycetes and evaluation of biofilm producing bacteria and A549 lung cancer cells. Journal of King Saud University-Science, 34(3), 101866. https://doi.org/10.1016/j.jksus.2022.101866
14. Nabila, M. I., & Kannabiran, K. (2018). Biosynthesis, characterization and antibacterial activity of copper oxide nanoparticles (CuO NPs) from Actinomycetes. Biocatalysis and Agricultural Biotechnology, 15, 56-62. https://doi.org/10.1016/j.bcab.2018.05.011
15. Bawazir, A. M. A., Shivanna, G. B., &Shantaram, M. (2018). Impact of Different Media for Growth and Production of Different Soluble Pigments in Actinomycetes Isolated from Soils of Hadhramout, Yemen. Eur. J. Biomed, 5, 615-619.
16. Li, Q., Chen, X., Jiang, Y., & Jiang, C. (2016). Morphological identification of Actinobacteria. Actinobacteria-basics and biotechnological applications, 59-86. https://doi.org/10.5772/61461
17. Ehinmitola, E. O., Aransiola, E. F., &Adeagbo, O. P. (2018). Comparative study of various carbon sources on rhamnolipid production. South African journal of chemical engineering, 26, 42-48. https://doi.org/10.1016/j.sajce.2018.09.001
18. Kejariwal, M., Tiwari, A., &Sahani, S. (2018). Development of Water Quality Field Testing Kit(WQFTKs)- A modified H2S Strip Test Method for detection of Hydrogen Sulfide Producing Bacteria. Advances in Bioresearch, 9, 146-154.
19. Mahima, P., Amridha, R., & V, P. S. (2020). Isolation, screening and identification of amylase and catalase producing bacterial strains from marine sediments. Indian Journal of Experimental Biology, 58, 853-860.
20. Elbendary, A. A., Hessain, A. M., El-Hariri, M. D., Seida, A. A., Moussa, I. M., Mubarak, A. S.,& El Jakee, J. K. (2018). Isolation of antimicrobial producing Actinobacteria from soil samples. Saudi Journal of Biological Sciences, 25, 44-46. https://doi.org/10.1016/j.sjbs.2017.05.003
21. Cruz, J. A., Garcia, F. C., & Evangelista, E. V. (2017). Isolation, characterization andidentification of plant growth-promoting rhizobacteria. International Journal of Agricultural Technology, 13, 715-727.
22. Kosco, J., Gonzalez-Carrero, S., Howells, C. T., Fei, T., Dong, Y., Sougrat, R., ...& McCulloch, I. (2022). Generation of long-lived charges in organic semiconductor hetero junction nanoparticles for efficient photocatalytic hydrogen evolution. Nature Energy, 7(4), 340-351. https://

doi.org/10.1038/s41560-022-00990-2
23. Yassin, M. T., Mostafa, A. A. F., Al-Askar, A. A., & Al-Otibi, F. O. (2022). Synergistic Antibacterial Activity of Green Synthesized Silver Nanomaterials with Colistin Antibiotic against Multidrug-Resistant Bacterial Pathogens. Crystals, 12(8), 1057. https://doi.org/10.3390/cryst12081057
24. Yilmaz, M. T., Ispirli, H., Taylan, O., &Dertli, E. (2021). A green nano-biosynthesis of selenium nanoparticles with Tarragon extract: Structural, thermal, and antimicrobial characterization. LWT, 141, 110969. https://doi.org/10.1016/j.lwt.2021.110969
25. Ismail, M. I. M. (2020). Green synthesis and characterizations of copper nanoparticles. Materials Chemistry and Physics, 240, 122283. https://doi.org/10.1016/j.matchemphys.2019.122283
26. Kayalvizhi, S., Sengottaiyan, A., Selvankumar, T., Senthilkumar, B., Sudhakar, C., & Selvam,K. (2020). Eco-friendly cost-effective approach for synthesis of copper oxide nanoparticles for enhanced photocatalytic performance. Optik, 202, 163507. https://doi.org/10.1016/j.ijleo.2019.163507
27. Singh, J., Kumar, V., Kim, K., & Rawat, M. (2019). Biogenic synthesis of copper oxide nanoparticles using plant extract and its prodigious potential for photocatalytic degradation of dyes. Environmental Research, 177, 108569. https://doi.org/10.1016/j.envres.2019.108569
28. Chaieb, K., Kouidhi, B., Jrah, H., Mahdouani, K., &Bakhrouf, A. (2011). Antibacterial activity of Thymoquinone, an active principle of Nigella sativa and its potency to prevent bacterial biofilm formation. BMC Complementary and Alternative Medicine, 11, 29. https://doi.org/10.1186/1472-6882-11-29
29. Zhang, E., Li, F., Wang, H., Liu, J., Wang, C., Li, M., & Yang, K. (2013). A new antibacterial titanium-copper sintered alloy: Preparation and antibacterial property. Materials Science and Engineering: C, 33, 4280-4287. https://doi.org/10.1016/j.msec.2013.06.016
30. Veneu, D. M., Torem, M. L., & Pino, G. A. H. (2013). Fundamental aspects of copper and zinc removal from aqueous solutions using a Streptomyces lunalinharesii strain. Minerals Engineering, 48, 44-50. https://doi.org/10.1016/j.mineng.2012.11.015
31. Kirova, G., Velkova, Z., &Gochev, V. (2012). Copper (II) removal by heat inactivated Streptomyces fradiae biomass: Surface chemistry characterization of the biosorbent. Journal of BioScience and Biotechnology, 2012, 77-82.
32. Lin, Y., Wang, X., Wang, B., Mohamad, O., & Wei, G. (2012). Bioaccumulation characterization of zinc and cadmium by Streptomyces zinciresistens, a novel Actinomycete. Ecotoxicology and Environmental Safety, 77, 7-17. https://doi.org/10.1016/j.ecoenv.2011.09.016
33. Sriramulu, M., Shanmugam, S., &Ponnusamy, V. K. (2020). Agaricus bisporus mediated biosynthesis of copper nanoparticles and its biological effects: An in-vitro study. Colloid and Interface Science Communications, 35, 100254. https://doi.org/10.1016/j.colcom.2020.100254
34. Bukhari, S. I., Hamed, M. M., Al-Agamy, M. H., Gazwi, H. S. S., Radwan, H. H., &Youssif, A.M. (2021). Biosynthesis of Copper Oxide Nanoparticles Using Streptomyces MHM38 and Its Biological Applications. Journal of Nanomaterials, 2021, 1-16. https://doi.org/10.1155/2021/6693302
35. Kouhkan, M., Ahangar, P., Babaganjeh, L. A., & Allahyari-Devin, M. (2020). Biosynthesis of Copper Oxide Nanoparticles Using Lactobacillus casei Subsp. Casei and its Anticancer and Antibacterial Activities. Current Nanoscience, 16, 101-111. https://doi.org/10.2174/1573413715666190318155801
36. Natesan, K., Ponmurugan, P., Gnanamangai, B. M., Manigandan, V., Joy, S. P. J., Jayakumar, C., & Amsaveni, G. (2020). Biosynthesis of silica and copper nanoparticles from Trichoderma, Streptomyces and Pseudomonas spp. evaluated against collar canker and redroot-rot disease of tea plants. Archives of Phytopathology and Plant Protection, 0, 1-30. https://doi.org/10.1080/03235408.2020.1817258
37. Hassan, Saad EL-Din, Salem, S. S., Fouda, A., Awad, M. A., El-Gamal, M. S., &Abdo, A. M.(2018). New approach for antimicrobial activity and bio-control of various pathogens by biosynthesized copper nanoparticles using endophytic Actinomycetes. Journal of Radiation Research and Applied Sciences, 11, 262-270. https://doi.org/10.1016/j.jrras.2018.05.003
38. Hassan, Saad El-Din, Fouda, A., Radwan, A. A., Salem, S. S.,Barghoth, M. G., Awad, M. A., El-Gamal, M. S. (2019). Endophytic Actinomycetes Streptomyces spp mediated biosynthesis of copper oxide nanoparticles as a promising tool for biotechnological applications. JBIC Journal of Biological Inorganic Chemistry, 24, 377-393. https://doi.org/10.1007/s00775-019-01654-5
39. Rathore, D. S. (2019). Isolation strategies, abundance and characteristics of the marine Actinomycetes of Kachhighadi, Gujarat, India. Journal of the Marine Biological Association of India, 61, 71-78. https://doi.org/10.6024/jmbai.2019.61.1.2028-11
40. Tesche, S., Rösemeier-Scheumann, R., Lohr, J., Hanke, R., Büchs, J., &Krull, R. (2019).Salt-enhanced cultivation as a morphology engineering tool for filamentous Actinomycetes:Increased production of labyrinthopeptin A1 in Actinomaduranamibiensis. Engineering in Life Sciences, 19, 781-794. https://doi.org/10.1002/elsc.201900036
41. Gohel, S. D., & Singh, S. P. (2017). Morphological, Cultural and Moleculardiversity of The Salt-Tolerant Alkaliphilic Actinomycetes from Saline Habitats. In Microbial Biotechnology Technological Challenges and Developmental Trends Vol. 1, pp. 337-354. https://doi.org/10.1201/b19978-22
42. Hassan, Saad EL-Din, Salem, S. S., Fouda, A., Awad, M. A., El-Gamal, M. S., &Abdo, A. M.(2018). New approach for antimicrobial activity and bio-control of various pathogens bybiosynthesized copper nanoparticles using endophytic Actinomycetes. Journal of Radiation Research and Applied Sciences, 11, 262-270. https://doi.org/10.1016/j.jrras.2018.05.003
43. Kumar, T., Chandrasekar, M., Senthilkumar, K., Ilyas, R. A., Sapuan, S. M., Hariram, N., ...& Siengchin, S. (2021). Characterization, thermal and antimicrobial properties of hybrid cellulose nanocomposite films with in-situ generated copper nanoparticles in Tamarindus indica Nut Powder. Journal of Polymers and the Environment, 29(4), 1134-1142. https://doi.org/10.1007/s10924-020-01939-w
44. Benassai, E., Del Bubba, M., Ancillotti, C., Colzi, I., Gonnelli, C., Calisi, N., &Ristori, S.(2021). Green and cost-effective synthesis of copper nanoparticles by extracts of non-edible and waste plant materials from Vaccinium species: Characterization and antimicrobial activity. Materials Science and Engineering: C, 119, 111453. https://doi.org/10.1016/j.msec.2020.111453
45. Sharma, A., & Dutta, R. K. (2015). Studies on the drastic

improvement of photocatalytic degradation of acid orange-74 dye by TPPO capped CuO nanoparticles in tandem with suitable electron capturing agents. RSC Advances, 5, 43815-43823. https://doi.org/10.1039/C5RA04179A

46. Raheem, R. A., Al-Gubury, H. Y., Aljeboree, A. M., &Alkaim, A. F. (2016). Photocatalytic degradation of reactive green dye by using Zinc oxide. Journal of Chemical and Pharmaceutical Sciences, 9, 1134-1138.
47. Salar, R. K., Kumar, J., & Kumar, S. (2012). Isolation and Evaluation of Fungal Strains from Textile Effluent Disposal Sites for Decolorization of various Azo Dyes. TerrAquat Environ Toxicol, 6, 96-99.
48. Thakare, R. U. (2020). Decolorization of dyes with immobilized laccase. BIOINFOLET-A Quarterly Journal of Life Sciences, 17(3b), 504-506.
49. Cao, S., Wang, J., Chen, H., & Chen, D. (2011). Progress of marine biofouling and antifouling technologies. Chinese Science Bulletin, 56, 598-612. https://doi.org/10.1007/s11434-010-4158-4
50. Lobelle, D., &Cunliffe, M. (2011). Early microbial biofilm formation on marine plastic debris. Marine Pollution Bulletin, 62, 197-200. https://doi.org/10.1016/j.marpolbul.2010.10.013